210

EVALUATION OF THE COUPLING POTENTIAL IN CLOSED-CELL LAMINATED COMPOSITES FOR ROTORCRAFT

Sean Muder, Robert Haynes, and Erian Armanios
University of Texas at Arlington
701 Nedderman Dr., Arlington, 76019, USA
sean.muder@mavs.uta.edu

ABSTRACT

A variational asymptotic beam analysis code is utilized to examine the extension-twist coupling and torsional and bending stiffness properties of box beams constructed from hygrothermally stable stacking sequences optimized for extensions-twist coupling in a flat strip configuration. The stiffness and compliance coefficients are compared for configurations containing optimized extension-twist coupled sequences and a Winckler-type sequence. The majority of the optimized sequences with the exception of the nine-ply sequence did not demonstrate higher levels of extension-twist coupling than the Winckler-type sequence.

INTRODUCTION

Laminated fiber-reinforced composite materials provide designers with the flexibility to create structures that have coupling between in-plane and out-of-plane deformation modes [1]. This behavior would be advantageous in the blade structure of a tilt-rotor aircraft. The twist distribution in the blade of a tilt-rotor aircraft that provides optimal power is different for the vertical and forward flight regimes [2]. Past and ongoing research suggests that the ideal distributions can be achieved by implementing passive blade control through extension-twist coupling.

In a flat strip, extension twist coupling occurs as a result of in-plane extension shear coupling associated with plies that have their fibers running off axis to the loading direction. A laminate with plies that shear in opposite directions above and below the mid-plane would produce opposing shearing forces on the bottom and top half of the laminate cross section, thereby producing a twisting moment that yields out-of-plane twisting deformation [3], as illustrated in Fig. 1.

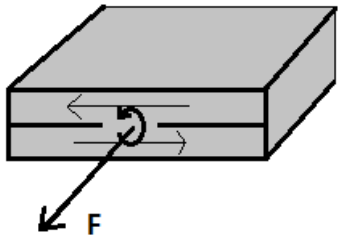

FIG 1. Extension Twist Coupling in Flat Strip

The most basic stacking sequence that incorporates extension-twist coupling is given by the angle ply laminate $[\pm\theta]$ [4]. Laminates with extension-twist coupling, such as the angle-ply laminate often exhibit hygrothermal instabilities, which cause the laminate to warp out-of-plane with temperature or moisture changes. In rotor blade application these hygrothermal instabilities are typically undesirable. A stacking sequence of the form $[\theta/(\theta-90)_2/\theta/-\theta/(90-\theta)_2/-\theta]$ was proposed by Winckler [5] to eliminate the hygrothermal instability while retaining the extension-twist coupling behavior. Recently, new families of hygrothermally stable stacking sequences were developed that have optimal extension twist coupling in a flat strip configuration [6]. Distinct

stacking sequences reported for 5 to 10 plies provide more flexibility to the design process. Most notably is the fact that they have significantly higher levels of extension-twist coupling than the Winckler type stacking sequences.

To meet rotor blades' bending and torsional stiffness requirements, a closed-cell section configuration is considered in this investigation and represented by the box beam shown in Fig. 2. The aim is to determine if the gains achieved by the hygrothermally stable stacking sequences for flat strips [6] hold for closed-cell sections. Extension-twist coupling can be created in a closed-cell section by wrapping a laminate exhibiting in-plane extension-shear coupling around a mandrel, as depicted in Fig. 2. This configuration has a circumferentially uniform stiffness and has been referred to as such in [7].

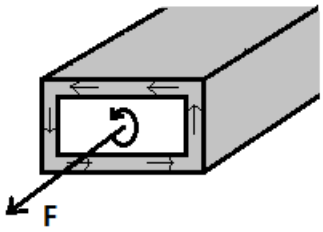

FIG 2. Extension Twist Coupling in Box Beam

Previous work has been conducted to analyze the stiffness properties of closed-cell sections composed of Winckler-type sequences. It is noted that there is a decrease in the level of extension twist coupling with an increase in the torsional stiffness of the section [8]. The necessity of adequate levels of bending stiffness required for rotor-blade application and the subsequent use of closed-section beams results in a high torsional stiffness, and thus restricts the usefulness of extension-twist coupling for passive blade control. The higher levels of extension twist coupling in the recently developed optimized sequences have the potential for increasing the level of extension-twist coupling while maintaining hygrothermal stability.

PROCEDURE

The variational asymptotic method was utilized in previous work by Berdichevsky *et al* [7] to develop an equation for strain energy density for slender closed-cell sections in terms of four kinematic parameters λ_1, κ_1, κ_2, and κ_3 as

$$\begin{aligned}\Phi=\frac{1}{2}\left[C_{11}\lambda_1^2+C_{22}\kappa_1^2+C_{33}\kappa_2^2+C_{44}\kappa_3^2\right]\\ +C_{12}\lambda_1\kappa_1+C_{13}\lambda_1\kappa_2+C_{14}\lambda_1\kappa_3\\ +C_{23}\kappa_1+C_{24}\kappa_1\kappa_3+C_{34}\kappa_2\kappa_3\end{aligned} \quad (1)$$

where λ_1, κ_1, κ_2, and κ_3 represent the axial strain along the 1 axis and curvatures about the 1, 2, and 3 axes respectively. This equation can be differentiated in terms of the kinematic parameters to formulate the constitutive relationships, Eq. (2). These relate the axial force, twisting moment, and bending moments to the corresponding four kinematic variables. The approximation neglects the transverse shear deformation and is valid when the ratio of the wavelength of the deformation to the characteristic diameter of the cross section remains large [9]. Closed-cell slender beams inherently maintain this ratio. The resulting stiffness matrix is given as

$$\begin{Bmatrix} F_1 \\ M_1 \\ M_2 \\ M_3 \end{Bmatrix} = \begin{bmatrix} C_{11} & C_{12} & C_{13} & C_{14} \\ C_{12} & C_{22} & C_{23} & C_{24} \\ C_{13} & C_{23} & C_{33} & C_{34} \\ C_{14} & C_{24} & C_{34} & C_{44} \end{bmatrix} \begin{Bmatrix} \lambda_1 \\ \kappa_1 \\ \kappa_2 \\ \kappa_3 \end{Bmatrix} \quad (2)$$

and by inverting Eq. (2), the compliance coefficients can be obtained as

$$\begin{Bmatrix} \lambda_1 \\ \kappa_1 \\ \kappa_2 \\ \kappa_3 \end{Bmatrix} = \begin{bmatrix} S_{11} & S_{12} & S_{13} & S_{14} \\ S_{12} & S_{22} & S_{23} & S_{24} \\ S_{13} & S_{23} & S_{33} & S_{34} \\ S_{14} & S_{24} & S_{34} & S_{44} \end{bmatrix} \begin{Bmatrix} F_1 \\ M_1 \\ M_2 \\ M_3 \end{Bmatrix} \quad (3)$$

The Variational Asymptotic Beam Sectional Analysis (VABS) [10] is used in this work to analyze the stiffness properties of box beam configurations composed of optimal stacking sequences. The code simplifies the nonlinear three-dimensional analysis of slender structures into a two dimensional cross sectional analysis and a one dimensional beam analysis.

The coordinate system referred to throughout the study is shown in Fig. 3; x_1 denotes the axis that runs parallel to the length of the beam and x_2 and x_3 are the local Cartesian coordinates of the cross section.

FIG. 3 Coordinate system

Using a finite element mesh of the desired cross section that contains all of the material and geometric properties of the section, the code generates asymptotically correct 4x4 stiffness and compliance matrices that describe the structural properties of the beam, as shown in Eqs. (2) and (3), respectively.

Of interest in this work is extension-twist coupling governed by S_{12}. It relates the twisting curvature, κ_1, to the applied axial force, F_1.

Table 1: Material Properties

Material Properties:

Moduli of Elasticity	Shear Moduli	Poisson's Ratio
E_1 = 125 GPa	$G_{12} = G_{13}$ = 4.3 GPa	$\upsilon_{12} = \upsilon_{13} = \upsilon_{23}$ =.328
$E_2 = E_3$ = 8.45 GPa	G_{23} = 3.4 GPa	

Geometric Properties:

Wall thickness = 1.216 mm	Avg. width = 100 mm	Avg. Height = 50 mm

Table 1 lists the material and geometric properties of the box beam that were used to conduct the study in [6]. Figure 4 illustrates the geometry of the cross section.

In order to ensure the accuracy of the results yielded by the VABS code, a convergence study was conducted to determine the necessary number of nodes and elements in the mesh to a value within 0.1% difference. The laminate sequence used for the study corresponds to the five-ply optimized laminate of Table 2. For a given number of nodes on each side of the box, S_{12} was extracted from the VABS output.

The results of the convergence study are shown in Figure 5. S_{12} increased by 0.0139% when the number of nodes on the side was increased from 1001 to 4001; therefore, 1001 nodes were used on each side.

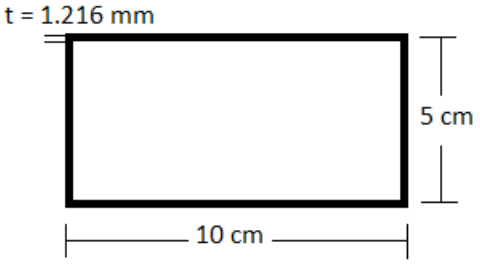

FIG 4. Convergence of S_{12} with increasing nodes on a side.

The dimensions of the box beam shown in Fig 4 were chosen within a range of typical spar sizes for rotor aircraft and remain constant throughout the analysis. The material properties are provided in Table 1.

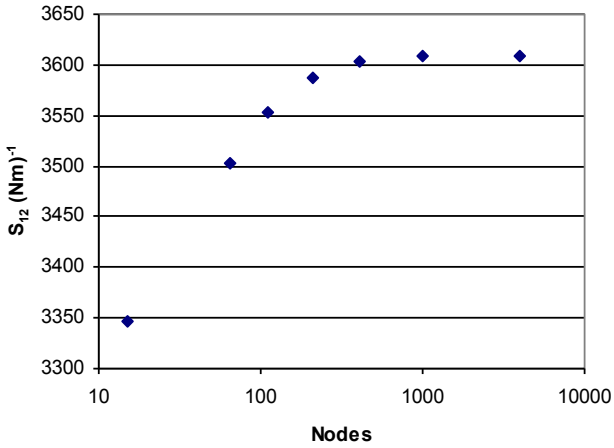

FIG 5. Box Beam Dimensions

The optimized stacking sequences in Table 2 were introduced into the box beam configuration to investigate their influence on extension-twist coupling.

Table 2: Optimal Stacking Sequences:

Type	Stacking Sequence
5 Ply	[-58.7/11.4/45/78.6/-31.3]
6 Ply	[21.2/-63.8/-48.7/48.7/63.8/-21.2]
7 Ply	[14.1/-76.9/-73.9/45/-16.1/-13.2/75.7]
8 Ply	[-21.5/72.1/57.9/-29.6/29.6/-57.9/-72.1/21.5]
9 Ply	[25.5/-79/32.5/-62.9/49.9/27.4/57/-10.6/64.9]
10 Ply	[16.2/-69.0/-65.3/31.8/42.1/-42.1/-31.8/65.3/69.0/-16.2]
Winckler	$[22.5/-67.5_2/22.5/-22.5/67.5_2/-22.5]$

In the first part of the investigation the thickness of each individual ply was calculated as 1.216mm divided by the number of plies in the stacking sequence in order to reduce the effect of changing geometry on the

predictions. As a result the total wall thickness was kept constant.

The trapeze effect, which takes into consideration the nonlinear contribution of axial force to the twisting curvature, was not included in this study. Its contribution is significant in torsionally soft open section beams [11]. The high torsional rigidity of the box beam makes the trapeze contribution negligible [9].

The mesh for the box beam cross section was developed using a preprocessor program written in Mathematica. In accordance with the convergence study the mesh used for the code contained 1001 nodes in the horizontal dimension of the beam and 1001 elements in the vertical direction.

In the second part of this study, the ply thickness was maintained constant as 0.152mm.

RESULTS

Figures 6 and 7 present the absolute values for S_{12} and C_{12}, respectively, for all optimal stacking sequences and the Winckler-type laminate when the total wall thickness is held constant. Note that "W" stands for the Winckler-type laminate. Only the nine-ply optimal stacking sequence outperforms the Winckler-type laminate. The coefficient of variance among all laminates is 10.4% and 14.2% for S_{12} and C_{12}, respectively, suggesting that changing stacking sequence has little effect on coupling. This can be explained by noting that the extension twist coupling compliance, S_{12} and torsional stiffness C_{22} are governed by the enclosed area of a closed-section slender beam as shown by their closed form expressions [12]. For a circumferentially uniform stiffness layup Eq. (2) simplifies to

$$\begin{Bmatrix} F_1 \\ M_1 \\ M_2 \\ M_3 \end{Bmatrix} = \begin{bmatrix} C_{11} & C_{12} & 0 & 0 \\ C_{12} & C_{22} & C_{23} & 0 \\ 0 & 0 & C_{33} & 0 \\ 0 & 0 & 0 & C_{44} \end{bmatrix} \begin{Bmatrix} \lambda_1 \\ \kappa_1 \\ \kappa_2 \\ \kappa_3 \end{Bmatrix} \tag{4}$$

and leads to the following closed-form expressions for C_{22} and S_{12}

$$C_{22} = \frac{C}{l} A_e^2$$
$$S_{12} = \frac{B}{\left(B^2 - AC\right)A_e} \tag{5}$$

where

$$A = A_{11} - \frac{A_{12}^2}{A_{22}}$$
$$B = 2\left(A_{16} - \frac{A_{12}A_{26}}{A_{22}} \right) \tag{6}$$
$$C = 4\left(A_{66} - \frac{A_{26}^2}{A_{22}} \right)$$

with A_e denoting the enclosed area and l the circumferential length. The in-plane stiffness coefficients are denoted in Eqs. (6) by A_{ij} [1].

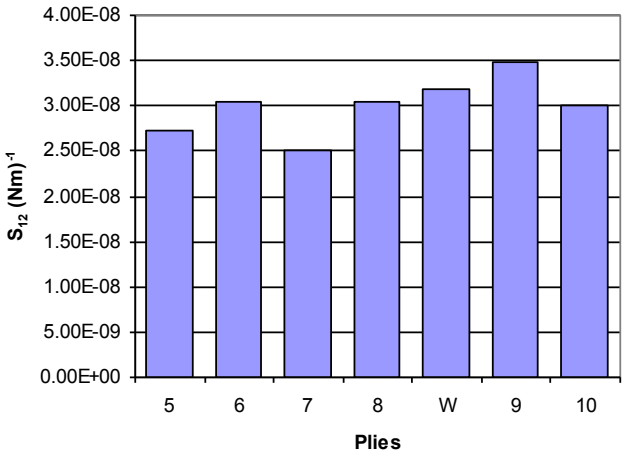

FIG 6. Extension-twist Coupling Compliance

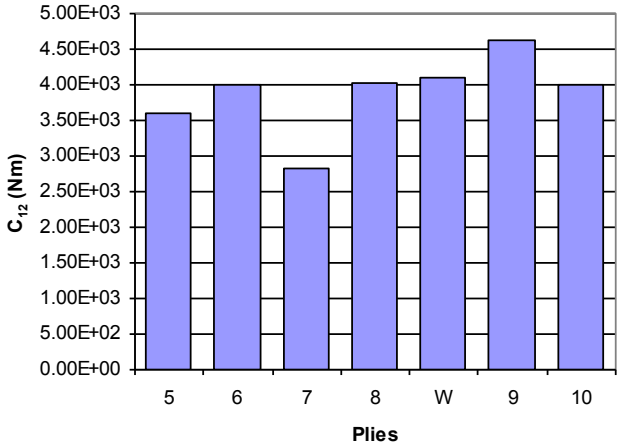

FIG 7. Extension-twist Coupling Stiffness

For the case when the ply thickness is maintained constant, the absolute values for S_{12} and C_{12} are provided in Figs. 8 and 9, respectively. The extension-twist coupling stiffness is expressed as

$$C_{12} = BA_e \qquad (7)$$

The coefficient of variance among all laminates is 13.9% and 52.4% for S_{12} and C_{12}, respectively. The values for S_{12} are very close to those for the case when total wall thickness is maintained. However, there is a clear linear trend in C_{12}, which follows from a comparison with isotropic thin-walled structures in which the torsional stiffness is proportional to the wall thickness. .

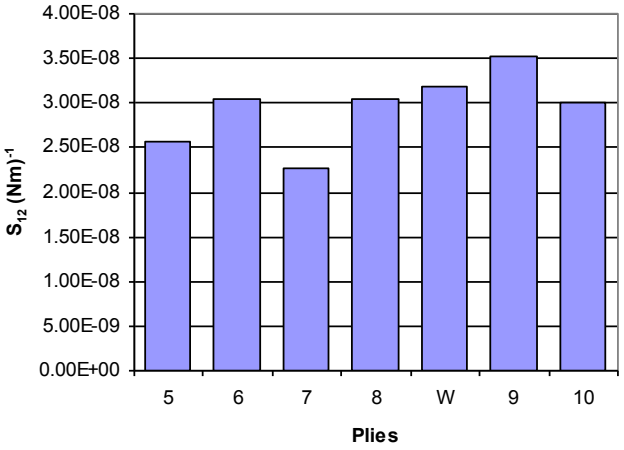

FIG 8. Extension-twist Coupling Compliance

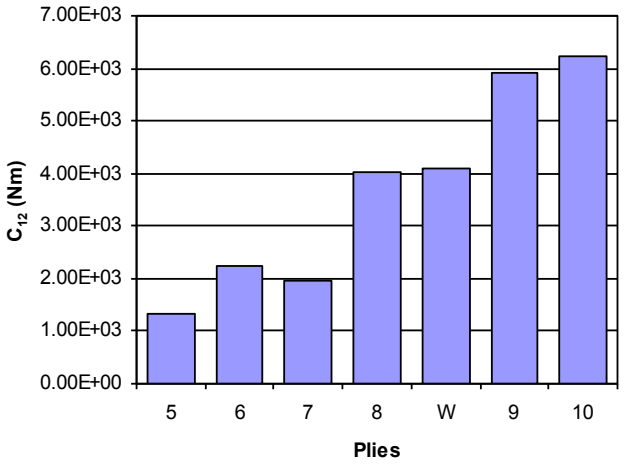

FIG 9. Extension-twist Coupling Stiffness

Table 3 provides the torsional and bending stiffnesses and compliances as obtained from VABS. As expected, the stiffnesses increase with ply count. The most notable exception is the seven-ply laminate, which has an exceptionally high stiffness and low compliance, making it a suboptimal choice for achieving extension-twist coupling.

Table 3. Torsional and Bending Stiffnesses

Plies	C_{22} (Nm^2)	S_{22} $(Nm^2)^{-1}$	C_{33} (Nm^2)	S_{33} $(Nm^2)^{-1}$	C_{44} (Nm^2)	S_{44} $(Nm^2)^{-1}$
5	5142	$1.94\cdot10^{-4}$	4896	$2.04\cdot10^{-4}$	13983	$7.15\cdot10^{-5}$
6	7115	$1.41\cdot10^{-4}$	5038	$1.98\cdot10^{-4}$	14390	$6.95\cdot10^{-5}$
7	4921	$2.03\cdot10^{-4}$	8520	$1.17\cdot10^{-4}$	24332	$4.11\cdot10^{-5}$
8	8363	$1.20\cdot10^{-4}$	7700	$1.30\cdot10^{-4}$	21986	$4.55\cdot10^{-5}$
W	7351	$1.36\cdot10^{-4}$	8507	$1.18\cdot10^{-4}$	24295	$4.12\cdot10^{-5}$
9	9610	$1.04\cdot10^{-4}$	8501	$1.18\cdot10^{-4}$	24273	$4.12\cdot10^{-5}$
10	10906	$9.17\cdot10^{-5}$	9240	$1.08\cdot10^{-4}$	26370	$3.79\cdot10^{-5}$

CONCLUSIONS

A finite element beam analysis code was used to determine the level of extension-twist coupling and torsional and bending stiffnesses and compliances in optimized stacking sequences introduced into a box beam configuration. In the first case, the geometric properties of the beam were held constant and hygrothermally stable stacking sequences optimized for extension-twist coupling were introduced into the configuration. Only the nine-ply optimal stacking sequence outperformed the Winckler-type stacking sequence in compliance. In the second case, the ply thickness was held constant. While the extension-twist coupling stiffness increased with ply count, the compliance did not decrease appreciably. Again, only the nine-ply stacking sequence outperformed the Winckler-type laminate.

The optimal stacking sequences in a closed-section box configuration did not outperform Winkler to the extent shown in their flat strip configuration. Currently, an investigation is being conducted into configurations that produce optimal extension-twist coupling in closed-section box configurations as well as other configurations, such as star beams and modified star beams.

REFERENCES

[1] Jones, R.M., 1999. *Mechanics of Composite Materials,* Taylor and Francis, PA, USA.

[2] Nixon, M.W., 1998. “Improvements to Tilt Rotor Performance Through Passive Blade Twist Control,” NASA TM-100583.

[3] Inn, K, 2003. “Development and Analysis of Elastically Tailored Composite Star Shaped Beam Sections,” PhD Thesis, School of Aerospace Engineering, Georgia Institute of Technology.

[4] Hyer, M.W. 1982. “The Room temperature Shapes of Four-layer Unsymmetric Cross-ply Laminates,” *Journal of Composite Materials,* 16(4): 318-340.

[5] Winckler, S.J., 1985. “Hygrothermally Curvature Stable Laminates with Tension torsion Coupling,” *Journal of the American Helicopter Society,* 30(3): 56-58.

[6] Haynes, R.A, Armanios, EA., 2010. “New Families of Hygrothermally Stable Composite Laminates with Optimal Extension-twist Coupling,” *AIAA Journal,* 48(12): 2954-2961.

[7] Berdichevsky, V., Armanios, E. A., Badir, A., 1992. “Theory of Anisotropic Thin Walled Closed Cross Section Beams," Composites Engineering, Vol. 2, No. 5-7, pp. 411-432.

[8] Serkan, O., 2006. “Extension Twist Coupling in Composite Rotor blades,” PhD Thesis, School of Aerospace Engineering, Georgia Institute of Technology.

[9] Bauchau, O. A., Hodges, D. H., 1999. “Analysis of Nonlinear Multi-Body Systems with Elastic Couplings,” Multibody System Dynamics, Vol 3, pp. 168-188.

[10] Yu, W, 2001. “VABS Manual for Users,”, pp. 1-3.

[11] Armanios, E. A., Makeev, A., and Hooke, D. A., 1996. "Finite-Displacement Analysis of Laminated Composite Strips with Extension-twist Coupling" J. Aerosp. Engrg., ASCE, Vol. 9, No. 3, July, 1996, pp. 80-91

[12] Armanios, E.A., and Badir, A.M., 1995. “Free Vibration Analysis of Anisotropic Thin-Walled Closed-Section Beams,” AIAA Journal, 33(10): 1905-1910.